Primary and Secondary Glyoxal Formation from Aromatics: Experimental Evidence for the Bicycloalkyl−Radical Pathway from Benzene, Toluene, and *p*-Xylene

R. Volkamer,*,† U. Platt,‡ and K. Wirtz†

Centro de Estudios Ambientales del Mediterraneo, C. Charles R. Darwin 14, 46980 Paterna, Valencia/Spain, and Institut für Umweltphysik, University of Heidelberg, INF 229, 69120 Heidelberg, Germany

Received: January 16, 2001; In Final Form: May 16, 2001

A new approach is presented to study the ring-cleavage process of benzene, toluene, and *p*-xylene (BTX). DOAS (differential optical absorption spectroscopy) was used for the simultaneous measurement of the respective ring-retaining products as well as glyoxal (a ring-cleavage product) in a series of experiments at the EUPHORE outdoor simulation chamber, Valencia/Spain. The good time resolution of the DOAS measurements (1−2 min) allowed the primary formation of glyoxal to be separated from any further contributions through additional pathways via reactions of stable intermediate compounds (secondary glyoxal formation). The ring-retaining products and glyoxal were identified as primary products. The primary glyoxal yield was found to be essentially identical to the overall yield of glyoxal formed over the time scale of the experiments. The negligible contribution from secondary glyoxal formation pathways was quantitatively understood for the experimental conditions of this study and was found to be representative for the troposphere. The yield of glyoxal was determined to be 35% ± 10% for benzene and about 5% higher for toluene and *p*-xylene. For benzene, the yield of hexadienedial was estimated to be ≤ 8%. It is concluded that ring-cleavage pathways involving the bicycloalkyl radical are major pathways in the oxidation of monocyclic aromatic hydrocarbons, i.e., BTX. The branching ratio for the bicycloalkyl radical intermediate, proposed to form from the reaction of the aromatic−OH adduct with atmospheric oxygen, could be directly identified with the primary glyoxal yield for the benzene system and as a lower limit in the case of toluene and *p*-xylene. Implications for the chemical behavior of aromatic hydrocarbons in the atmosphere are discussed.

Introduction

The OH-radical addition reaction to the aromatic ring of benzene, toluene, or xylenes results in the formation of a hydroxycylclohexadienyl radical (and its methylated derivates), also termed aromatic−OH adduct. Under atmospheric conditions, the aromatic−OH adduct will react primarily with oxygen.[1] Presently, five intermediate species are postulated to form from this reaction (see Figure 1): (1) phenol-type compounds, (2) a peroxy radical,[2,3] (3) a bicycloalkyl radical,[2,4] (4) an epoxide-alkoxy radical,[2] and (5) areneoxides.[5]

To date, little is known about the branching ratio for the formation of the different intermediates (if, indeed, all of them are formed). This is due in part to difficulties in the direct observation of the highly reactive intermediates in the experiment.[5,6] Recent progress has been made in the quantification of the phenol-type compounds[7−11] (1). Nevertheless, considerable uncertainty exists with regard to the branching ratio of the highly reactive intermediates (2−5). Though the presently available product data[12−16] are consistent with all four of these intermediates,[6,14] their indirect identification through observable stable products is not straightforward, because in principle a given product may be formed through different pathways. Even for compounds such as glyoxal, which are known to be significant products of the OH-reaction of aromatic compounds,[9,12,13,17,18] definite formation pathways have not yet been established.

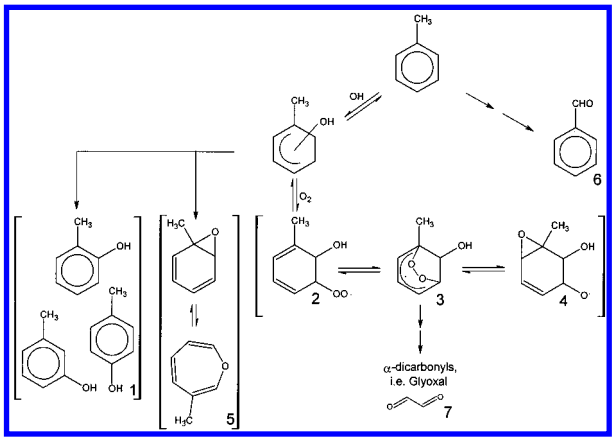

Figure 1. Initial steps of the OH radical initiated oxidation of toluene. The OH radical may either abstract an H atom from the side chain or add to the aromatic ring. The aromatic−OH adduct formed in the latter case can react with molecular oxygen to yield one of the five proposed intermediate compounds (see text). Analogous intermediates are proposed for benzene and *p*-xylene.

Thus, mechanistic conclusions from the yield of glyoxal are not straightforward, but rather require the separation of primarily formed glyoxal from glyoxal formed from the further reaction of stable intermediate compounds (secondary glyoxal). With the use of differential optical absorption spectroscopy (DOAS),[19−21] we demonstrate here that this separation has become possible.

* To whom correspondence should be addressed. Present address: Institut für Umweltphysik, University of Heidelberg, INF 229, 69120 Heidelberg, Germany. Phone: +49 6221 546527. Fax: +49 6221 546405. E-mail: rainer.volkamer@iup.uni-heidelberg.de.

† Centro de Estudios Ambientales del Mediterraneo.

‡ University of Heidelberg.

10.1021/jp010152w CCC: $20.00
Published on Web 07/31/2001

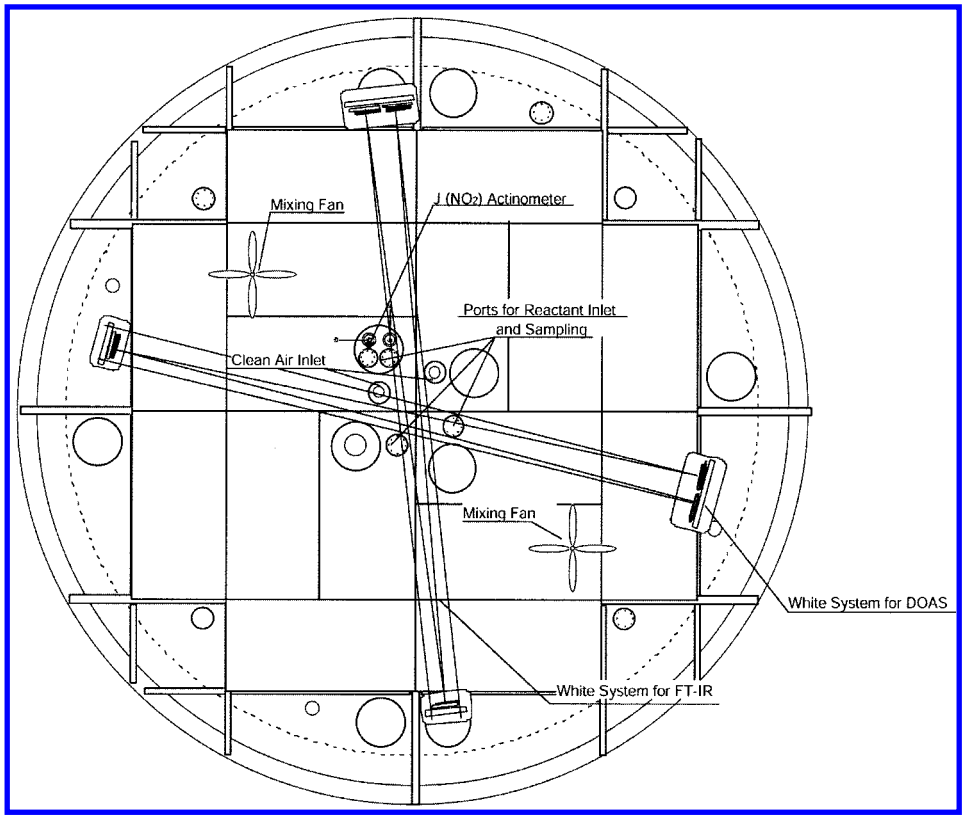

Figure 2. Top view of one of the outdoor simulation chambers (EUPHORE chamber A) at CEAM Institute, Valencia/Spain.

Indications for Fast Ring-Cleavage from Aromatics in the Literature. Until now, experimental indications of fast ring-cleavage have been derived from two studies on *o*-xylene.[14,22] Both studies investigate the formation of biacetyl, a C_4-α-dicarbonyl that is formed only from *o*-xylene and not from other aromatic compounds.[23] Darnall et al.[22] observed the biacetyl with a time-resolution of 30 min and postulated the formation of the bicycloalkyl radical intermediate to explain the observed concentration time profile of biacetyl. Nevertheless, primary products observed at time scales of tens of minutes may be difficult to distinguish from secondary products formed from highly reactive stable intermediate species, and these measurements cannot rule out the involvement of such intermediates.[6] Even though time-resolution is not a limitation with the API-MS (atmospheric pressure ionization mass spectrometry) measurements of Kwok et al.,[14] the data reported are qualitative only. Furthermore, the API-MS technique is limited to observing biacetyl as only α-dicarbonyl compound because of problems of the technique with the detection of low molecular weight molecules;[14] hence, it is restricted to investigation of the *o*-xylene system.

The highly time-resolved, simultaneous DOAS detection of ring-retaining products (intermediates 1 and 6 in Figure 1) and glyoxal (7 in Figure 1) in our smog-chamber studies eliminates these limitations because glyoxal is formed from almost any aromatic system, i.e., benzene, toluene, and *p*-xylene.

Experimental Section

In this study, three experiments were carried out at the large-volume outdoor smog chamber EUPHORE,[8,24] located in Valencia/Spain. EUPHORE consists of two hemispherical chambers with an approximate volume of 187 m^3. The chambers are made of 120 μm thick FEP foil, highly transmittive for visible as well as UV light (transmittance in the visible is approximately 85−90%; at 290 nm it is still about 75%). The aluminum floor panels of the chamber, covered with FEP sheet, can be water-cooled to prevent solar heating of the chamber during the experimental runs, thus, maintaining realistic atmospheric temperature conditions for the course of an experiment. Two mixing fans of 67 m^3 min^{-1} air throughput are mounted inside the chamber to ensure homogeneous mixing of the volume. An air purification and drying system provides NO_y−, NMHC-free, and dry air, allowing the background concentration of NMHC species to be as low as 0.3 μg m^{-3} (equivalent to about 0.5 ppbC). A hydraulically controlled steel housing protects the chamber from sunlight and weather.

A top view of the EUPHORE chamber used in this study is shown in Figure 2. Inside this chamber two White-type multireflection cells are mounted, one coupled to an FTIR interferometer and the other to the DOAS spectrometer. The White system coupled to FTIR is equipped with gold-coated mirrors and was operated at an absorption path length of 326.8 m. The FTIR interferometer (NICOLET Magna 550, MCT detector) was operated to yield spectra of 1 cm^{-1} spectral resolution with 280 scans coadded, yielding a time resolution of 5 min. The actively laser-aligned White system coupled to the DOAS was operated with UV-enhanced aluminum-coated mirrors (Alflex-UV, Balzers, Liechtenstein) at an absorption path length of 386 m. A 500 W Xe-high-pressure arc lamp was used as light source. The f/6.9 Czerny Turner spectrograph (ACTON 500; focal length, 0.5 m) was thermostated to $T = 30$ °C and operated at a spectral resolution (fwhm) of 0.84 nm (grating, 300 grooves/mm; blaze, 300 nm). The linear photodiode array detector (Hamamatsu, 1024 diodes, Hoffmann Messtechnik, Rauenberg) flange mounted to the spectrograph was cooled by a dual-stage Peltier element with a forced-air-cooled heat sink to $T = -20$ °C in order to reduce dark current to less than 0.8% of the signal. Spectra were sequentially recorded at two spectral intervals, (1) 246−411.8 nm and (2) 387−552.8 nm, yielding an overall time-resolution of the DOAS measurements

of about 2 min. Periodically, a straylight spectrum was recorded for each spectral interval by either introducing a long-pass filter GG475, 3 mm thickness (Schott Glaswerke, Mainz), into the lightbeam or blocking the latter. All of the measured spectra were corrected for stray light, dark current, and electronic offset.[25] Absorption structures from molecular oxygen which interferes with the aromatic absorption signal at wavelengths below 290 nm were eliminated by dividing the respective spectra by a reference spectra recorded the same day in the clean air of the flushed reactor volume.[20] If not mentioned explicitly, the calibration of DOAS and FTIR was performed using literature cross-sections.[21]

Installed in addition to these instruments were two J_{NO2} filter radiometers (one measuring direct sunlight and one facing downward to measure reflected light from the floor panels), sampling ports for an ozone monitor (Monitor Labs ML9810), a NO_x monitor (ECO Physics CLD 770AL) with a photolytic converter (PLC 760), a hygrometer (Walz TS-2), and a GC (Hewlett-Packard 6890) with flame ionization detector (FID). Floor and air temperatures inside the chamber were measured with two PT-100 thermocouples. Ozone, NO_x, temperature, radiation, and humidity data were collected and saved in a data acquisition system.

In each of the three runs, a predetermined amount of a single aromatic compound (benzene, toluene, or *p*-xylene) was introduced into the chamber using a calibrated syringe. Initial concentrations of benzene, toluene, and *p*-xylene were about 1025, 860, and 750 ppb (1 ppb $= 2.46 \times 10^{10}$ molec cm^{-3} at 298 K), respectively. Nitrous acid was generated by a liquid-phase reaction of sodium nitrite with diluted sulfuric acid. The mixtures of HONO, NO, and NO_2 produced by this reaction were transferred directly into the chamber by a stream of purified air. Some NO was added to delay the formation of ozone in the system. Initial concentrations of HONO, NO, and NO_2 were 80, 80, and 40 ppb, respectively. The reactants were allowed to mix for at least 30 min before exposing the chamber to sunlight. To keep the chamber inflated, purified dry air was added to compensate for system leakage. The dilution was measured following the decay of SF_6, an initially added (25ppb) inert tracer, by means of FTIR.

The decay of the aromatic compounds was monitored every 4 min by GC-FID, using a HP-5, cross-linked 5% PHME silicone 30 m $\times$ 0.32 mm $\times$ 0.25 μm column, and the relative data was subsequently cross-calibrated through the initial concentration of the aromatic compound as determined by FTIR. DOAS was used for the detection of products, i.e., phenol (benzene system); benzaldehyde, *o*-, *m*-, and *p*-cresol (toluene system); *p*-tolualdehyde and 2,5-dimethylphenol (*p*-xylene system); as well as HONO, NO_2, formaldehyde, and glyoxal (in any system) at a time-resolution of 1−2 min. Only the data of relevance to this study are presented here.

Even though the UV absorption cross-section of glyoxal is not well-known at present, the uncertainties influence the differential cross-section (σ') only to a minor extent.[21,26] The main uncertainties are due to the saturation effects of individual lines measured at our rather low spectral resolution (0.84 nm fwhm) which result in distortions in the apparent absorption cross-section spectra bands. Line-shape changes were eliminated by recording a reference spectrum of glyoxal prior to the experiments using the same apparatus as that for the measurements. Calibration was performed from simultaneously recorded FTIR spectra using the IR cross-section from Moortgat et al. (personal communication). Nevertheless, the remaining uncertainty in the σ' is estimated to be rather of the order of several 10% and cannot explain the observed differences in the glyoxal yield. An error of 20% was included in the uncertainty of the average yield given in Table 1. A confirmation of the glyoxal absorption cross-section is desirable.

Results

The experimental data obtained from the *p*-xylene system are shown as an example in Figure 3. The concentration−time profiles of *p*-xylene, the ring-retaining products (p-tolualdehyde and 2,5-dimethylphenol), and glyoxal are shown together with J_{NO2} values. The steep rise in J_{NO2} corresponds to the opening of the chamber housing; later variations are due to passing clouds. By the time the maximum glyoxal concentration was reached, almost clear sky conditions prevailed. The decay in *p*-xylene before the opening of the chamber housing was due to dilution (indicated by a dashed line). After opening the chamber housing, OH radicals were generated from the photolysis of nitrous acid. The concentrations of glyoxal and the ring-retaining products were observed to build up quickly, and in fact, all these compounds were detected in the very first DOAS spectra after the opening of the chamber housing. Further on, the *p*-tolualdehyde concentration was found to steadily increase, reaching a plateau of about 10 ppb. The concentration of glyoxal was found to increase steadily up to a distinct maximum mixing ratio of 62 ppb at about 11:50 GMT. The maximum concentration of glyoxal was reached when the net production rate (production rate minus loss rates) of glyoxal was zero; that is, the steady-state concentration of glyoxal had been reached. Afterward, the glyoxal concentration was found to drop until the end of the experiment, with photolytic loss of glyoxal gaining importance with decreasing reactivity in the reaction system and thus in the glyoxal formation rate (12:15 GMT). A somewhat different concentration time profile was observed for 2,5-dimethylphenol. After an initial increase, the 2,5-dimethylphenol concentration reached a maximum concentration of about 7 ppb and then dropped to about half that value, remaining constant until the end of the experiment. This deviation in the 2,5-dimethylphenol concentration-time profile with respect to those of *p*-tolualdehyde and glyoxal can be explained by the formation of NO_3 radicals in the reaction system. The daytime reaction of NO_3 radicals with phenol-type compounds is known to act as an effective phenol sink in smog-chamber experiments[8,27] and has also been suggested as a process for removing phenols from the daytime atmosphere.[10,28] The NO_3 radical concentration was estimated following the approach described in ref 8. The formation of NO_3 radicals is directly related to ozone formation in the system. Ozone was effectively suppressed through the added NO during the initial phase of an experiment. In the later phase of an experiment, NO_3 radical concentrations reached calculated levels of $\leq$ 2.5 ppt.[8,10] For the phenol type compounds, the fast reaction with NO_3 radicals under these conditions becomes an important sink. As is discussed below, only the phenol formation during the initial phase of the benzene experiment is relevant to the outcome of this study. It is unaffected by the reaction with NO_3 radicals. Loss due to reaction with NO_3 radicals is further found to be negligible for glyoxal and the aldehydes because of the slow reaction of these species with NO_3. Hence, the reactions of NO_3 radicals could be neglected in the further evaluation.

Evaluation of the Glyoxal Yields. Recommended OH-reaction rate constants (*k* values) of glyoxal and the aromatics were used.[23] The photolysis frequency J_{gly} for glyoxal was estimated from J_{NO2} on the basis of the relation[29] $J_{gly} = 0.0105 J_{NO2}$. Corrections for product (i.e., glyoxal, p-tolualde-

TABLE 1: Φ Yield of Glyoxal from the Oxidation of Benzene, Toluene, and *p*-Xylene

compound	$P_{glyoxal}/P_{pro}$ [rel. units]	$\Phi_{glyoxal,t=o}$ [%]	$\Phi_{glyoxal,SS}$ [%]	$\Phi_{product}$ [%]	literature (no. of the reference list)
			Benzene		
phenol				23.6 ± 4.4	31
				23 ± 7	32
				25 ± 5	33
				51.0 ± 3.8	11
glyoxal				20.7 ± 1.9	18
	0.685 ± 0.013	**34.9 ± 3.9**[1]	**35.5 ± 6.6**	**35.2 ± 9.6**	this work[a]
			Toluene		
benzaldehyde				5.8 ± 0.8	8
				6.0 ± 0.6	7
				5.9 ± 0.6	reference yield (average)
glyoxal				8.0 ± n.n.	49
				11.1 ± 1.3	51
				9.8 ± n.n.	52
				15.0 ± 4.0	53
				10.5 ± 1.9	18
				20.3 ± n.n.	47
				23.8 ± 2.5	7
	6.78 ± 0.20	**40.0 ± 4.2**	**37.9 ± 6.5**	**39.0 ± 10.2**	this work
			p-Xylene		
p-tolualdehyde				8.0 ± 1.3	17
				7.0 ± 1.0	34
				6.4 ± 1.5	35
				10.3 ± 1.6	9
				8.1 ± 1.3	10
				8.0 ± 1.0	reference yield (average)
glyoxal				12.0 ± 2.0	51
				24 ± 2	17
				22.5 ± 3.9	18
				39.4 ± 11.0	9
	5.29 ± 0.08	**42.3 ± 5.3**	**38.4 ± 7.0**	**40.4 ± 10.6**	this work

[a] Glyoxal yield calculated on the basis of the phenol yield from ref 11.

hyde, etc.) loss through OH-reaction and photolysis were calculated from eq 1a

$$[\text{product}]_{\text{corrected}} = [\text{product}]_{\text{measured}} F \qquad (1a)$$

$$F = 1 + [\text{product}]_{\text{lost}}/[\text{product}]_{\text{measured}} \qquad (1b)$$

The amount of product lost via secondary reactions, i.e., $[\text{product}]_{\text{lost}}$ in eq 1b, was calculated from eq 2:

$$[\text{product}]_{\text{lost}} = \int (k_{\text{OH}}(\text{product})[\text{OH}] + J_{\text{product}})[\text{product}]_{\text{measured}}\, \mathrm{d}t \qquad (2)$$

The decay of the aromatic compound was used to estimate the concentration of OH radicals, yielding typical OH levels of about 5×10^6 molec cm^{-3}. Under these conditions, the photolytic loss of glyoxal is comparable to that through reaction with OH radicals, and both processes need to be corrected for. The ring-retaining products are essentially lost through OH reaction. Photolysis of the aromatic aldehydes as well as deposition of the products, i.e., phenolic compounds, to the chamber walls are minor loss processes here and were neglected in the further evaluation.

The concentration−time profiles of the ring-retaining products and glyoxal were evaluated to determine the glyoxal yields at different times during each experiment. Two approaches were followed.

First, the glyoxal yield was determined relative to the yields of the ring-retaining products. For not-too-high product concentrations, the production rate of the products was essentially unaffected by product loss processes. At the time-resolution of the DOAS system, the initial three to seven data points after opening the chamber housing were essentially not influenced by OH losses ($F < 1.1$, eq 1b). To be able to include more data points in the analysis, it was decided to account for secondary loss of products. In Figure 4, the glyoxal mixing ratio is plotted against the respective ring-retaining products from benzene (Figure 4a; $F_{\text{phenol}} < 1.7$, $F_{\text{glyoxal}} < 1.4$), toluene (Figure 4b; $F_{\text{benzaldehyde}} < 1.17$, $F_{\text{glyoxal}} < 1.13$), and *p*-xylene (Figure 4c; $F_{p-\text{tolualdehyde}} < 1.13$, $F_{\text{glyoxal}} < 1.1$). From Figure 4a−c, the ratios of the glyoxal production rate relative to that of the respective

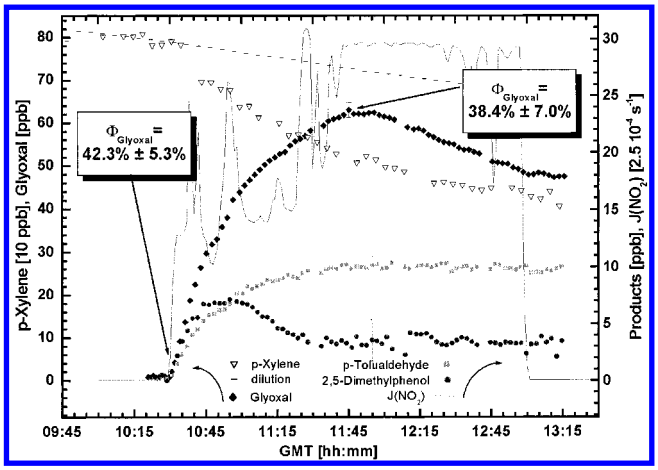

Figure 3. Concentration−time profile determined in the oxidation of *p*-xylene (triangles): the ring-retaining products, *p*-tolualdehyde (squares) and 2,5-dimethylphenol (dots), are formed simultaneously with the ring-cleavage product glyoxal (diamonds). Both compounds are observed in the very first spectra after opening the chamber. Two approaches were followed to determine the yield of glyoxal with a certain time resolution. Also shown are J_{NO2} (solid line) and SF_6 (dashed line), added as dilution tracer.

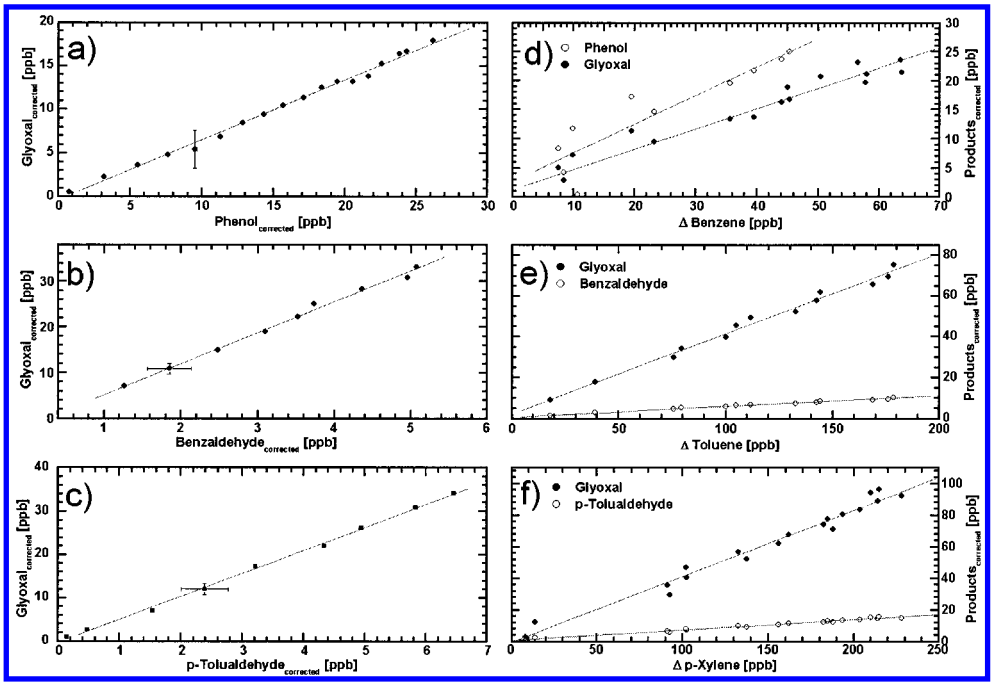

Figure 4. Plot of the glyoxal mixing ratios, corrected for reaction with OH radicals and photolysis (see text; a−c) vs the ring-retaining compound produced over the first couple of hours of reaction time and (d−f) vs the amount of reacted aromatic compound for the benzene, toluene and *p*-xylene system.

ring-retaining product were determined from a least-squares fit to the data. The ratios obtained are given in Table 1 and can be identified with the ratio of the yields of both compounds. The glyoxal yield at the very beginning of each experiment ($\Phi_{\text{glyoxal},t=0}$ in Table 1), i.e., within the first 5−10 min, was hence calculated by multiplying this ratio with the respective yield of the corresponding ring-retaining product included in Table 1. In the case of the alkyl-substituted benzenes, the respective aldehyde compound was used as a reference compound, with the "reference yield" being determined as the average of the available literature values.

Second, the sum of the primary and secondary glyoxal formed through a sequence of stable intermediate compounds was determined for benzene, toluene, and *p*-xylene after about 90 min of reaction time when the glyoxal concentration time profile showed a well characterized maximum concentration, indicating that a steady-state concentration had been reached. The overall yield of glyoxal was hence calculated from eq 3:

$$\Phi_{\text{glyoxal}} = \frac{(k_{\text{gly}}[\text{OH}] + J_{\text{gly}})[\text{gly}]}{k_{\text{aro}}[\text{OH}][\text{aro}]} \qquad (3)$$

Concentrations of glyoxal and the parent aromatic compound were measured, and the concentration of OH radicals was traced from the aromatic species decay rate averaged 15 min before and after the maximum concentration of glyoxal considering dilution and the *k* value of the respective aromatic compound. The overall yield of glyoxal determined from eq 3 is given as $\Phi_{\text{glyoxal,SS}}$ in Table 1.

Observations. From the experimental data, all of the observed products were identified as primary products. This is illustrated in Figure 4 (right column) where the amounts of glyoxal ($F <$ 1.6) and a respective ring retaining product ($F <$ 1.55) are plotted against the reacted amount of benzene (Figure 4d), toluene (Figure 4e), and *p*-xylene (Figure 4f), as determined from the GC-FID data after correction for dilution. The given data points were correlated to match the sampling time of the GC and cover about 90 min of reaction time. A fixed relation (i.e., straight line) was observed for the amount of ring-retaining product and glyoxal formed from a given amount of aromatic hydrocarbon.

These two methods for calculating glyoxal yields allow the primary glyoxal yield to be separated from the secondary glyoxal that may be formed through further reaction of stable intermediate compounds. Interestingly, the primary and secondary yields of glyoxal were found to be essentially identical within the experimental errors, as can be seen in Table 1 and Figure 4d−f. Consequently, we conclude that the secondary formation of glyoxal is only of minor importance under the experimental conditions of our study.

Discussion

Time-Scale for Product Formation. The OH-radical abstraction reaction with alkyl-substituted aromatic compounds is known to lead to the formation of aldehyde-type compounds[30] (intermediate 6, Figure 1). The reaction sequence of this abstraction reaction is well understood, and in the presence of NO (only a few ppb), it is expected to form aldehyde-type compounds at close-to-unity yield. From the reaction sequence shown in Figure 1, the NO-to-NO_2 conversion reaction is expected to be the rate-limiting step under atmospheric conditions. Nevertheless, in the presence of 2 ppb of NO the delay in the formation of the aldehyde will be as small as a few seconds. Initial concentrations of NO in this study were in the range of several tens of ppbs, and the aldehyde-type compounds were formed less than a second after the initial OH-radical attack on the side chain. Hence, the aldehydes are observed as primary products.

Phenol-type compounds (intermediate 1, Figure 5) are reported as primary products for benzene,[11,18,31−33] toluene,[7,8,31] and *p*-xylene.[9,10] The formation of phenols was observed to be direct, i.e., to be consistent with the reaction aromatic−OH + $O_2 \rightarrow$ phenol + HO_2, for toluene[8] and *p*-xylene.[10] The delay resulting from this reaction for phenol formation under atmospheric conditions is of the order of milliseconds, and accordingly, phenol is observed as a primary product.

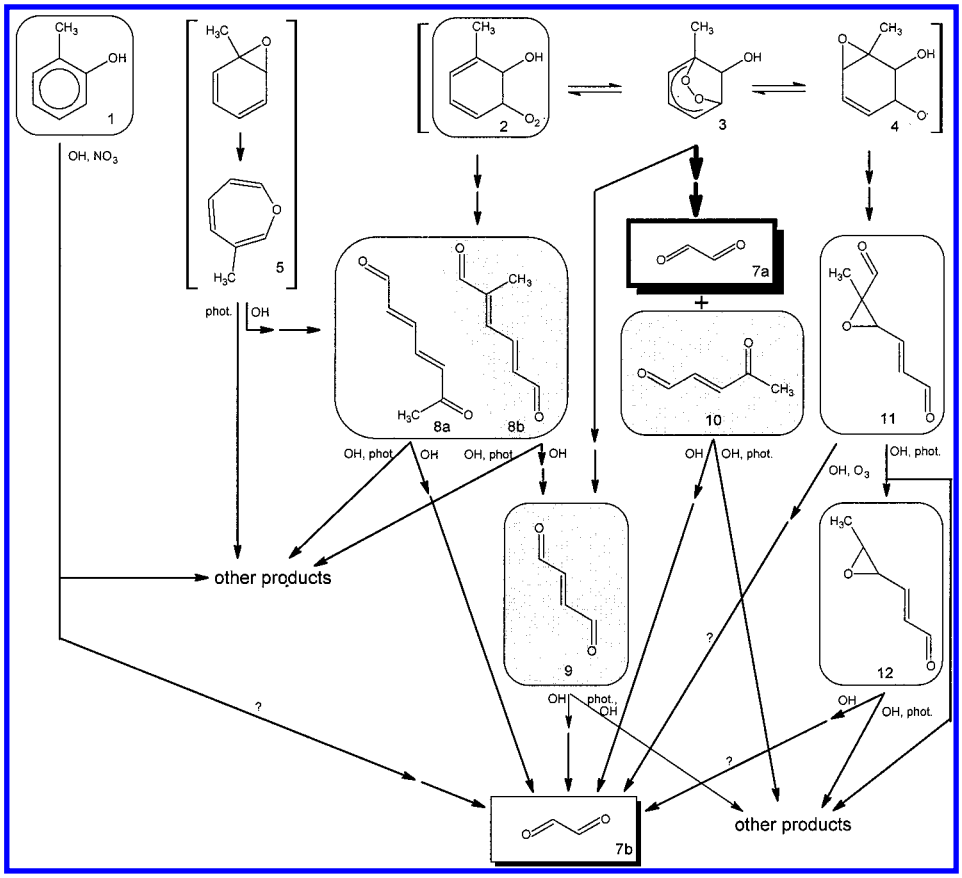

Figure 5. Possible pathways for the formation of glyoxal (shaded boxes) from toluene. In principle, any intermediate compound (Figure 1) may result in the formation of glyoxal as primary, secondary, or higher-generation product. The identified formation of primary glyoxal involving the bicycloalkyl radical is highlighted by the thick arrows. Experimentally identified products (round-edged boxes) and products that have been demonstrated to yield glyoxal (shaded background) are shown. Similar schemes can be adapted for other aromatic compounds.

TABLE 2: Kinetic Parameters of Dicarbonyl-Type Products from BTX

	photolysis-rate J $[10^{-5}\ s^{-1}]^a$	OH−rate constant k_{OH} $[cm^3\ mol^{-1}s^{-1}]$	photolyt. lifetime [min]	OH-lifetime[b] [min]	overall lifetime [min]	relative OH-loss [%]
butenedial	134[c]	5.2×10^{-11}[d]	12.4	64	10.3	16
4-oxo-2-pentenal	162[e]	5.6×10^{-11}[d]	10.3	59.5	8.8	15
2-methyl-butenedial[f]	134	5.2×10^{-11}	12.4	64	10.3	16
3-hexene-2,5-dione	4.3[g]	5.9×10^{-11}[d]	390	61	51.5	86
E,Z-2,4-hexadienedial	111[h]	7.4×10^{-11}[h]	15	45.1	11.3	25
E,E−2,4-hexadienedial	9.2[i]	7.6×10^{-11}[h]	180	43.9	35.3	81
E,E−2-methyl-2,4-hexadienedial	9.2[j]	11.8×10^{-11}[j]	180	28.3	21.5	87
glyoxal	7.9[k]	1.15×10^{-11}[l]	210	290	122	42

[a] Scaled to $J_{NO2} = 7.5\ 10^{-3}\ s^{-1}$, representative for the experiments. [b] Calculated on the basis of $[OH] = 5\ 10^6$ molec cm^{-3}, representative for the experiments. [f] No kinetic data is available. The given data corresponds to that of butenedial (see text). [c] Based on ref 45: J(*cis*-butenedial)/J_{NO2}=0.18. [e] Based on ref 45: J(*cis*-4-oxo-2-pentenal)/J_{NO2}=0.22. [g] Based on ref 46: J(E/Z-3hexene2,5dione)/J_{NO2}=5.7 10^{-3}. [h] Reference 44; photolysis based on ref 44: J(EZ)/J_{NO2}=0.148. [i] Effective loss rate based on ref 44: J(EE)/J_{NO2}=0.0122. [j] *J*(*E,E*−2,4-hexadienedial) adapted; OH-rate constant from ref 43. [k] Based on ref 29: J(glyoxal)/J_{NO2}=0.0105. [d] Reference 13, for 3-hexene-2,5-dione an effective rate constant was calculated assuming a ratio of Z/E-isomers of 2/1 (ref 46). [l] Reference 56.

Glyoxal is also observed to be a primary product. From our good time-resolved detection of glyoxal, it is possible to draw conclusions about the operative ring-cleavage process of BTX, i.e., to assess the role of stable intermediate species. As possible loss processes of a hypothetical stable intermediate compound involved in glyoxal formation, photolysis and OH reaction need to be considered here. Likely glyoxal precursors are listed in Table 2 together with available kinetic data for photolysis and respective OH-rate constants. The fastest photolysis frequency from these compounds is $1.6 \times 10^{-3}\ s^{-1}$. Moreover, a fast (nearly collision rate limited) OH-radical reaction rate constant of $k = 1 \times 10^{-10}\ cm^3\ molec^{-1}\ s^{-1}$ may be assumed to estimate an upper limit of the loss rate through OH reaction of $1.0 \times 10^{-3}\ s^{-1}$ (based on an upper limit OH radical concentration in our system of 10^7 molec cm^{-3}). Hence, assuming both loss processes, a lower limit for the overall lifetime is obtained to be 385 s, i.e., 6−7 min. Any hypothetical in-this-way-delayed glyoxal formation would be observable at the time-resolution of our measurements. No delay is observed for the formation of glyoxal from benzene, toluene. and *p*-xylene as compared to the directly formed ring-retaining products (see Figure 4a−c), respectively. Consequently, no reaction pathway including the stable intermediates listed in Table 2 is fast enough to contribute to the observed primary yield of glyoxal.

Ring-Retaining Product Yields as "Reference Yields" for Glyoxal Yields. The reported overall yields of aldehyde-type compounds from toluene, i.e., benzaldehyde[7,8] and *p*-xylene, i.e., *p*-tolualdehyde,[9,10,17,34,35] are found to be constant over a wide

range of experimental conditions.[8,10] There exists little uncertainty in the yields of aldehyde-type compounds (see Table 1); therefore, the aldehyde yields of toluene and *p*-xylene are well suited as reference yields to quantify the yield of the direct formation of glyoxal.

With respect to the phenol yields, recent studies on toluene[7,8] and *p*-xylene[9,10] show excellent agreement for the yields of cresol isomers and 2,5-dimethylphenol, respectively. The phenol compounds nevertheless are considerably (about a factor of 4) more reactive toward the OH radical than the respective aldehyde-type compounds. This limits the use of phenols as a reference because the concentration-time profiles are affected by loss due to OH reaction already at a low phenol concentration. Consequently, the less reactive aldehyde-type compounds were chosen as reference compounds to determine the yield of glyoxal from toluene and *p*-xylene. For benzene, however, the only ring-retaining reference yield is that of phenol. This is not necessarily a limitation for this system. First, the DOAS technique is very sensitive to phenol (about a factor of 10 times more sensitive than for most other phenol-type compounds). Second, phenol is considerably less reactive than the methylated phenol-type compound with respect to the OH radical. Nevertheless, reported phenol yields fall basically into two groups. Several laboratory studies find phenol yields from the oxidation of benzene of about 24%.[31−33] A recent study using DOAS/FTIR for the phenol detection reports a twice as high phenol yield over a wide range of experimental conditions, i.e., down to benzene and, in particular, NO_x concentrations actually observed in the troposphere.[11] Further support for the high phenol yield comes from OH cycling experiments on benzene[36] that report a yield of "prompt" HO_2,[37] in agreement with these recent results. This discrepancy will be subject to a forthcoming paper.

For benzene, the high phenol yield of 51%[11] was used as a reference to calculate the yield for the direct formation of glyoxal given in Table 1. There are two reasons to use the high value: First, this yield was determined under experimental conditions comparable to those applied in this study. Second, the linear increase of glyoxal from benzene shown in Figure 4d indicates that secondary glyoxal formation is essentially negligible. Even though the data show considerable scatter due to the low conversion of benzene, the observed linear increase is only compatible with the observed high phenol yield (see Table 1).

A lower primary glyoxal yield as it would be calculated on the basis of a 24% phenol yield[31−33] is not in agreement with our observations.

Primary and Overall Yield of Glyoxal. At the time-resolution used for the detection of glyoxal in this study, the yield of glyoxal formed as a primary product (primary glyoxal) can be distinguished from other pathways that result in a delayed secondary formation of glyoxal.

A. Primary Yield of Glyoxal. The rapid glyoxal formation observed in this work is consistent with a reaction sequence involving the bicycloalkyl radical (intermediate 3, Figure 5) because glyoxal is formed from this pathway rapidly in a sequence of radical reactions without the involvement of stable intermediate compounds. The rate-limiting step for glyoxal formation from this sequence is supposed to be the conversion of the bicyclic peroxiradical to the bicyclic alkoxy radical through reaction with NO.[16,38] This reaction here is not expected to delay the formation of glyoxal significantly (<2 s). Assuming this reaction to be the only fate of the bicyclic peroxiradical,[16,38] it will result in the formation of α-dicarbonyls, i.e., glyoxal as primary products, and the primary yield of glyoxal can be identified as a quantitative indicator for the formation yield of the bicycloalkyl radical intermediate (3) formed from the reaction of the aromatic−OH adduct with oxygen. The direct yield of glyoxal determined in this study is high in any investigated system (see Table 1), indicating that fast ring cleavage, involving the bicycloalkyl radical intermediate, is a major operative ring-cleavage pathway for aromatic hydrocarbons, i.e., BTX.

B. Overall Yield of Glyoxal. The overall yield of glyoxal determined after approximately 90 min of reaction time was found to be essentially identical to the primary glyoxal yield for all of the three investigated systems. Hence, no significant indication for any secondary formation of glyoxal through the further reaction of stable intermediate compounds was observed. This result is further confirmed by the data shown in Figure 4 (right column) where the linear increase observed for glyoxal reflects the insignificant secondary contributions to the overall yield of glyoxal from BTX.

It is concluded that the glyoxal observed in this study from benzene, toluene, and *p*-xylene can be explained solely in terms of a primary formation of glyoxal. Any secondary sources of glyoxal are found to be of minor importance under conditions of relevance for the atmosphere.

Glyoxal Formation from Proposed/Observed Intermediate Species. In Figure 5, several possible pathways resulting in the formation of glyoxal are shown for the toluene system. In principle, all five intermediates (1−5) formed from the reaction of the toluene−OH adduct with oxygen may result in glyoxal, either as a primary product (7a) or a higher-generation product (7b). The experimentally identified products are shown in round-edged boxes, and the products that were demonstrated to yield glyoxal in the laboratory are shown on a shaded background. The thick arrows indicate the ring-cleavage pathway in agreement with the results of this study. Similar schemes can be adapted for the other aromatic compounds.

Phenols (1) are highly reactive toward the OH and NO_3 radical, and (as discussed above) the NO_3 radical reaction represents an operative removal pathway for phenols from the daytime atmosphere.[10,28] Nevertheless, the principal fate of phenol will be reaction with the OH radical, with the major primary products being dihydroxybenzenes, nitrophenols, and benzochinones.[39] Only a minor fraction (less than 10%) may undergo ring cleavage and thereby lead to the formation of glyoxal as a secondary product (7b).

The formation of a peroxy radical (2) was postulated in the late seventies,[22] but it took until recent years for tentative experimental evidence of its formation to be reported for the benzene system.[32] More recently, the existence of a peroxy radical has been proven experimentally, though indirectly, for benzene[36] and the toluene[40] system by cw UV-laser long-path absorption spectroscopy. The further fate of the peroxy radical may be intramolecular rearrangement[2] or reaction with NO. The reaction with NO may result in the formation of muconaldehydes (diunsaturated 1,6-dicarbonyls; 8a, 8b) as primary products.[16,41,42] The formation of glyoxal from muconaldehydes may proceed via OH reaction of the hexadienedials formed from benzene or the methyl-substituted derivatives of type (8a) formed from toluene and *p*-xylene. Moreover, the methyl-substituted derivatives of type (8b) may react with OH and form an unsaturated 1,4-dicarbonyl that under further OH attack may form glyoxal. This indirect glyoxal formation was demonstrated from the 2-methylhexa-2,4-dienedial (8b) to proceed through the further OH reaction of butenedial[43] (9). For both the muconaldehydes[44] and the unsaturated 1,4-dicarbonyl-type

products,[45,46] photolysis competes with OH reaction and only the OH-reaction of the latter yields glyoxal.

The bicycloalkyl radical (3) may form from the peroxy radical (2) through intramolecular 1,3-oxygen-bridge formation and has in fact been identified as one of the three likely intermediates to form on the basis of density function based calculations on the reaction of the toluene−OH adduct with oxygen.[2] The bicycloalkyl-type radicals can add additional O_2 and then react with NO to form the respective alkoxy radical. Alternative pathways are in principle possible[38] though considered nonoperative.[3,38] The alkoxy radical can further decompose in a sequence of two unimolecular decomposition steps into two radicals that subsequently yield an α-dicarbonyl (glyoxal from benzene; glyoxal and methylglyoxal for alkyl substituted aromatics) and an unsaturated 1,4-dicarbonyl compound (9 and 10), respectively, as primary products. The following 1,4-dicarbonyls of type (9 and 10) have been experimentally identified: butenedial[7,47] (9) and 4-oxo-pentenal[7,47,48] (10) from toluene, as well as 2-methyl-butenedial[9] and 3-hexene-2,5-dione[9,12,17,48] from *p*-xylene. For the unsaturated 1,4-dicarbonyl coproducts of glyoxal, photolysis competes with OH reaction. With the exception of 3-hexene-2,5-dione, the OH reaction of the unsaturated 1,4-dicarbonyls may contribute to the secondary formation of glyoxal.

The epoxide−alkoxy radical (4), the most stable of the three intermediate species proposed by Bartolotti and Edney,[2] may either form directly when oxygen is added to the ring or through intramolecular oxygen transfer from the peroxy radical.[2] As primary products, stable ring-retaining or stable long-chain (C_6 to C_8) ring-cleavage epoxide-type compounds (11) were proposed.[15] Experimentally, these compounds were tentatively identified in product studies on different alkylbenzenes including toluene[15] and *p*-xylene[14,15] with the molecular weights of the expected primary epoxide-type products matching the observed mass peaks from PFBHA-derivative GC/MS[15] and API-MS[14] analysis. However, positive quantitative confirmation of the formation of these compounds still requires standards. A secondary formation of glyoxal may result from the OH reaction or ozonolysis of type (11) epoxides.[15] Furthermore, these compounds may undergo photolysis and yield type (12) epoxide-type products.[15] Presumably, products of type (12) may further react with OH and also contribute to the secondary formation of glyoxal. From the aldehyde-type structure of these compounds, it is likely that, as in the case of the dicarbonyls, photolytic loss competes with OH reaction. However, little is known about the formation yield and principal fate of these epoxide-type compounds (11 and 12) in the atmosphere.

A second epoxide-type intermediate, benzeneoxide/oxepin, and its methylated derivatives, termed areneoxides (5), was postulated by Klotz et al.[5] The main difference between this pathway and the epoxide-alkoxy radical (4) pathway[2] is that a stable epoxide-type species (5) and additional "prompt HO_2" are formed as primary products of the reaction of the aromatic−OH adduct with oxygen. Apart from the tentative assignment of benzeneoxide/oxepin in the oxidation of benzene,[49] the areneoxides so far have not been observed experimentally.[32] Even though the OH reaction of benzeneoxide/oxepin[5] may result in the formation of the epoxide−alkoxy radical (4), the only products identified from this reaction are muconaldehydes (8a,b).[5] The further fate of the muconaldehydes and the pathways presumably leading to secondary glyoxal are discussed above.

Fate of Precursors for Secondary Glyoxal: Photolysis vs OH Reaction. As indicated in Figure 5, the principal fate of precursors for secondary glyoxal is either OH reaction or photolysis. Table 2 gives an overview of the available kinetic data for the OH reaction and photolysis of likely glyoxal precursors and glyoxal. The photolysis frequencies given were scaled relative to J_{NO2} to reflect the experimental conditions during the experiments, as described in the Table 2 legend.

For butenedial and the 4-oxo-pentenal, the measured values for the photolysis frequency[45] correspond to the cis isomers. In the following discussion, no difference for the trans isomer is assumed. Under our experimental conditions, photolysis was found to be extremely fast (photolytic lifetimes are only of the order of 10 min) for both compounds, dominating the OH reaction by a factor of 5. Only a small fraction of about 15% may undergo OH reaction and thereby yield some secondary glyoxal. Assuming unity yield for the glyoxal formation from this reaction, secondary glyoxal would still be in the range of the experimental error. Because the formation of maleic anhydrid is an alternative pathway of this reaction[13] the secondary glyoxal yield should be even lower.

The atmospheric chemistry of the 2-methyl-butenedial is unknown at present. Nevertheless, it is likely from the structural similarity of this compound with butenedial that photolysis will be the dominant fate in the presence of sunlight. Though the OH reaction may be faster than that of butenedial, the secondary yield of glyoxal from 2-methyl-butenedial is expected to be well below unity and thus should not significantly contribute to secondary glyoxal formation.

For 3-hexene-2,5-dione, the listed photolysis frequency[46] corresponds to an equilibrium mixture of *E*/*Z* isomers with a measured *E*/*Z* ratio of $^1/_2$. This ratio was used to estimate an effective OH reaction rate constant, given in Table 2. In addition, reaction with ozone may be of importance for the 3-hexene-2,5-dione.[50] On the basis of the ozonolysis rate constant $k_{O3} = 3.6 \times 10^{-18}$ cm^3 mol^{-1}s^{-1} and about 300 ppb of ozone, this pathway may contribute about 10% to the total loss of 3-hexene-2,5-dione, making reaction with OH its dominant fate. From the OH and O_3 reactions, however, methylglyoxal is expected to be formed primarily[13] and glyoxal is expected to be a minor product. In summary, secondary glyoxal formation from 3-hexene-2,5-dione should be insignificant.

The *E,Z*-2,4-hexadienedial in the presence of sunlight is found to rapidly isomerize into the *E,E* isomer.[44] From the described photolytic behavior of the *E,E*-2,4-hexadienedial,[44] loss through OH reaction will be the dominant removal process for this isomer under our experimental conditions. Hence, high yields of hexadienedials were expected to result in significant amounts of secondary glyoxal in the benzene system. The negligible secondary formation of glyoxal observed from benzene is thus an indicator that hexadienedials were not formed in significant amounts under our experimental conditions. From the experimental error of our measurements (6.6% for the overall glyoxal yield from benzene) an upper limit of the formation yield of hexadienedial-type compounds can be estimated to be ≤8%.

Similarly, the *E,E*-2-methyl-2,4-hexadienedial (8b in Figure 5) expected to form from toluene will primarily react with the OH radical yielding butenedial as primary product. Hence, the secondary formation of glyoxal from this compound should not be observable because of the rapid photolysis of butenedial under our experimental conditions.

Overall, the negligible contribution of secondary glyoxal observed from BTX can be understood from the rapid photolysis of the unsaturated 1,4-dicarbonyls. This result contrasts with the predictions made by state-of-the-art chemical models that

up to 40% of the glyoxal should be formed as secondary glyoxal. Possibly, photolysis is underestimated by these models.

Secondary glyoxal formation may, nevertheless, become important if under different experimental conditions OH reactions dominate over the photolytic loss of glyoxal precursors.

Comparison of the Glyoxal Yields to Literature Values. In Table 1, the glyoxal yields of this study (indicated $\Phi_{product}$) are compared to the available literature values. They are found to be comparable to the reported upper limit values or even above.[7,9,17,18,47,49,51−53] Excellent agreement is found for the *p*-xylene system, with the value of a recent study[9] being essentially identical to our results. Our values for benzene and toluene are considerably higher than reported literature values. However, comparing the glyoxal yields of the three systems to the respective literature values, no systematic discrepancy is observed. Hence, it is unlikely that the observed differences could be explained by systematic errors, i.e., the absorption cross section of glyoxal.

The uncertainty of the differential absorption cross section is estimated at 20% and dominates the error of the absolute quantity of the average glyoxal yields in Table 1. This uncertainty, however, only affects the absolute value of the glyoxal yield and cancels out if two yields are compared relatively. Hence, it is only of minor importance in this study. Nevertheless, a confirmation of the UV-absorption cross-section of glyoxal is desirable.

Implications for the Atmosphere. The fast ring-cleavage mechanism via the bicycloalkyl radical intermediate, identified as a major pathway for the oxidation of BTX in this study, effectively forms α-dicarbonyls. These compounds, as well as their expected unsaturated dicarbonyl-type coproducts, rapidly photolyze (see above) and are likely to represent significant radical sources.[54]

The impact on photooxidant formation in the troposphere requires a detailed analysis based on chemical modeling. Recent model results exist on 1,3,5-trimethylbenzene[55] for which the photochemical ozone creation potentials (POCP) of the five pathways were estimated starting from intermediate-type compounds comparable to (1−5) in Figure 1. The bicycloalkyl radical pathway is ascribed by far the highest POCP value. Hence, the high branching ratio identified for this pathway for the OH reaction of BTX is expected to lead to a significant increase in the photooxidant formation predicted by chemical models for BTX.

Furthermore, the high yield of the bicycloalkyl radical pathway may increase the importance of α-dicarbonyl-type compounds and their coproducts. This might be of relevance in investigations of mutagenic effects that were observed for the products of aromatic oxidation.[47]

Conclusions

Glyoxal is identified as a major primary product from the BTX−OH reaction, indicating that ring-cleavage pathways involving the bicycloalkyl radical are major operative pathways in the OH-initiated oxidation of aromatic compounds. The elementary reaction steps are as yet not fully elucidated. Most likely an α-dicarbonyl and a respective unsaturated 1,4-dicarbonyl-type coproduct are formed; other pathways are in principle possible[38] though considered nonoperative.[3,38] Hence, the primary glyoxal yield most likely is a marker for the bicycloalkyl radical pathway for benzene and gives a lower limit for the branching ratio of this pathway for the alkyl substituted aromatics.

Glyoxal formation from BTX is understood essentially in terms of primary glyoxal. The negligible contribution of pathways forming glyoxal through the OH reaction of stable intermediate compounds is probably due to the dominant photolysis of potential precursors for secondary glyoxal, i.e., unsaturated 1,4-dicarbonyl-type products. It underscores the importance of photolytic processes in the oxidation of aromatic hydrocarbons. The presently available unsaturated 1,4-dicarbonyl yields[7,9,12,17,47,48] are not corrected for photolytic loss and their redetermination is desirable. These yields are crucial to understand the fate of the bicycloalkyl radical and are likely to improve the poor carbon balance typical for aromatic systems. Further, the atmospheric chemistry of 2-methyl-butenedial is unknown at present.

The error of the absolute glyoxal yields determined in this study is dominated by the uncertainty of the UV-absorption cross-section (σ') of glyoxal. An improved determination of σ' is desirable.

Independent experimental evidence for the high phenol yield from benzene[11] is obtained.

BTX degradation schemes in chemical models need to be updated. The branching ratios of the bicycloalkyl radical need to reflect the high primary glyoxal yields. Furthermore, photolytic parameters need to reproduce the negligible secondary glyoxal yield.

Acknowledgment. Financial support from the European Commission within a Marie Curie research training grant under Contract No. ERB 4001GT970196 from the Environment and Climate Program, DG-XII is gratefully acknowledged. Further, Fundació BANCAIXA and the Generalidad Valenciana are acknowledged for their interest and financial support.

References and Notes

(1) Knispel, R.; Koch, R.; Siese, M.; Zetzsch, C. *Ber. Bunsen-Ges. Phys. Chem.* **1990**, *94*, 1375.
(2) Bartolotti, L. J.; Edney, E. O. *Chem. Phys. Lett.* **1995**, *245*, 119.
(3) Andino, J. M.; Smith, J. N.; Flagan, R. C.; Goddard, W. A.; Seinfeld, J. H. *J. Phys. Chem.* **1996**, *100*, 10967.
(4) Lay, T. H.; Bozzelli, J. W.; Seinfeld, J. H. *J. Phys. Chem.* **1996**, *100*, 6543.
(5) Klotz, B.; Barnes, I.; Becker, K. H.; Golding, B. T. *J. Chem. Soc., Faraday Trans.* **1997**, *93*, 1507.
(6) Atkinson, R. *Atmos. Environ.* **2000**, *34*, 2063.
(7) Smith, D. F.; McIver, C. D.; Kleindienst, T. E. *J. Atmos. Chem.* **1998**, *30*, 209.
(8) Klotz, B.; Sørensen, S.; Barnes, I.; Becker, K. H.; Etzkorn, T.; Volkamer, R.; Platt, U.; Wirtz, K.; Martín-Reviejo, M. *J. Phys. Chem.* **1998**, *102*, 10289.
(9) Smith, D. F.; Kleindienst, T. E.; McIver, C. D. *J. Atmos. Chem.* **1999**, *34*, 339.
(10) Volkamer, R.; Platt, U.; Ücker, J.; Wirtz, K. In *EUPHORE annual report 1998−1999*; Barnes, I., Brockmann, K., Eds.; FB9 Publishing: University of Wuppertal, Germany, 2001; 257−268.
(11) Volkamer, R.; Becker, K. H.; Klotz, B.; Platt, U.; Ücker, J.; Wirtz, K. In *Proc. Workshop on the Chem. Behaviour of Aromatic Hydrocarbons in the Troposphere*; Becker, K. H., Ed.; http://www.physchem.uni-wuppertal.de/PC−WWW_Site/workshops.html, Valencia, Spain, February 27th−29th, 2000; FB9 Publishing: University of Wuppertal, Germany; pp 15−23.
(12) Becker, K. H.; Klein, T. *Proceedings of the 4th European Symposium on the Physico-Chemical Behaviour of Atmospheric Pollutants*; Angeletti, G., Restelli, G., Eds.; Reidel Publishing: Dordrecht, The Netherlands, 1987; pp 320−326.
(13) Bierbach, A.; Barnes, I.; Becker, K. H.; Wiesen, E. *Environ. Sci. Technol.* **1994**, *28*, 715.
(14) Kwok, E. S. C.; Aschmann, S. M.; Atkinson, R.; Arey, J. *J. Chem. Soc., Faraday Trans.* **1997**, *93*, 2847.
(15) Yu, J.; Jeffries, H. E. *Atmos. Environ.* **1997**, *31*, 2281.
(16) Yu, J.; Jeffries, H. E.; Sexton, K. G. *Atmos. Environ.* **1997**, *31*, 2261.
(17) Bandow, H.; Washida, N. *Bull. Chem. Soc. Jpn.* **1985**, *58*, 2541.
(18) Tuazon, E. C.; MacLeod, H.; Atkinson, R.; Carter, W. P. L. *Environ. Sci. Technol.* **1986**, *20*, 383.

(19) Platt, U. *Air Monitoring by Spectroscopic Techniques*; Sigrist, Ed.; John Wiley & Sons: New York, 1994; pp 27−84.
(20) Volkamer, R.; Etzkorn, T.; Geyer, A.; Platt, U. *Atmos. Environ.* **1998**, *32*, 3731.
(21) Etzkorn, T.; Klotz, B.; Sørensen, S.; Patroescu, I. V.; Barnes, I.; Becker, K. H.; Platt, U. *Atmos. Environ.* **1999**, *33*, 525.
(22) Darnall, K. R.; Atkinson, R.; Pitts, J. N., Jr. *J. Phys. Chem.* **1979**, *83*, 1943.
(23) Atkinson, R. *J. Phys. Chem. Ref. Data* **1994**, *Monograph No. 2*, 1.
(24) *Final report "EUPHORE", European Commission Contract* EV5V-CT92-0059; Becker, K. H., Ed.; Commission of the European Communities: Brussels, Belgium, 1996.
(25) Volkamer, R. *Absorption von Sauerstoff im Herzberg I System und Anwendung auf Aromatenmessungen am European Photo Reactor (EUPHORE)*, Diplomarbeit D-491, Institut für Umweltphysik, University of Heidelberg, 1996.
(26) Stutz, J.; Kim, E. S.; Platt, U.; Bruno, P.; Perrino, C.; Febo, A. *J. Geophys. Res.* **1999**, *105*, D11, 14585.
(27) Carter, W. P. L.; Winer, A. M.; Pitts, J. N., Jr. *Environ. Sci. Technol.* **1981**, *15*, 829.
(28) (a) Ackermann, R.; Becker, K. H.; Geyer, A.; Gomes, J. A. G.; Kurtenbach, R.; Lörzer, J. C.; Platt, U. *Proc. Workshop on the Chem. Behaviour of Aromatic Hydrocarbons in the Troposphere*; Becker, K. H., Ed.; http://www.physchem.uni-wuppertal.de/PC-WWW_Site/workshops.html, Valencia, Spain, February 27th−29th, 2000; pp 124−130. (b) Kurtenbach, R.; Ackermann, R.; Becker, K. H.; Geyer, A.; Gomes, J. A. G.; Lorzer, J. C.; Platt, U.; Wiesen, P. *J. Phys. Chem.* **2001**, accepted for publication.
(29) Klotz, B.; Graedler, F.; Sørensen, S.; Barnes, I.; Becker, K. H. *Int. J. Chem. Kinet.* **2001**, *33*, 9.
(30) Finlayson-Pitts, B.; Pitts, J. N., Jr. *Atmsopheric Chemistry: Fundamentals and Experimental Techniques*; John Wiley & Sons: New York, 1986.
(31) Atkinson, R.; Aschmann, S. M.; Arey, J.; Carter, W. P. L. *Int. J. Chem. Kinet.* **1989**, *21*, 801.
(32) Bjergbakke, E.; Sillesen, A.; Pagsberg, P. *J. Phys. Chem.* **1996**, *100*, 5729.
(33) Berndt, T.; Böge, O.; Herrmann, H. *Chem. Phys. Lett.* **1999**, *314*, 435.
(34) Atkinson, R.; Aschmann, S. M.; Arey, J. *Int. J. Chem. Kinet.* **1991**, *23*, 77.
(35) Barnes, I.; Becker, K. H.; Bierbach, A.; Wiesen, E. In *Laboratory Studies on Atmospheric Chemistry*; Cox, R. A., Ed.; Air Pollution Research Report 42; Commission of the European Communities: Brussels, Belgium, 1991; pp 183−189.
(36) Bohn, B.; Zetzsch, C. *Phys. Chem. Chem. Phys.* **1999**, *1*, 5097.
(37) Siese, M.; Koch, R.; Fitschen, C.; Zetzsch, C. In *EUROTRAC Symp. 94*; Borrell, P. M., Borrell, P., Cvitas, T., Seiler, W., Eds.; Academic Publishing: The Hague, The Netherlands, 1994; pp 115−119.
(38) Atkinson, R.; Carter, W. P. L.; Darnall, K. R.; Winer, A. M.; Pitts, J. N., Jr. *Int. J. Chem. Kint.* **1980**, *12*, 779.
(39) Oliaru, R.; Barnes, I.; Becker, K. H.; Klotz, B.; Mocanu, R. In *Proc. of the EC/EUROTRAC-2 Joint Workshop*; Rossi, M. J., Rossi, E. M., Eds.; EPFL Publishing: Lausanne, Switzerland, September 11th−13th, 2000; pp 60−63.
(40) Bohn, B. *J. Phys. Chem.* **2001**, submitted.
(41) Hoshino, M.; Akimoto, H.; Okuda, M. *Bull. Chem. Soc. Jpn.* **1978**, *51*, 718.
(42) Dumdei, B. E.; O'Brien, R. J. *Nature* **1984**, *311*, 248.
(43) Klotz, B.; Bierbach, A.; Barnes, I.; Becker, K. H. *Environ. Sci. Technol.* **1995**, *29*, 2322.
(44) Klotz, B.; Barnes, I.; Becker, K. H. *Int. J. Chem. Kinet.* **1999**, *31*, 689.
(45) Sørenen, S.; Barnes, I. In *EUPHORE annual report*; Barnes, I., Wenger, J., Eds.; EPFL Publishing: Lausanne, Switzerland, 1997; pp 149−150.
(46) Graedler, F.; Barnes, I. In *EUPHORE annual report*; Barnes, I., Wenger, J., Eds.; EPFL Publishing: Lausanne, Switzerland, 1997; pp 146−148.
(47) Dumdei, B. E.; Kenny, D. V.; Shepson, P. B.; Kleindienst, T. E.; Nero, C. M.; Cupit, L. T.; Claxton, L. D. *Environ. Sci. Technol.* **1988**, *22*, 1493.
(48) Becker, K. H.; Barnes, I.; Bierbach, A.; Kirchner, F.; Thomas, W.; Wiesen, E.; Zabel, F. *EUROTRAC Annual Reports*, Part 8, LACTOZ.; Commission of the European Communities: Brussels, Belgium, 1992; pp 87−98.
(49) Shepson, P. B.; Edney, E. O.; Corse, E. W. *J. Phys. Chem.* **1984**, *88*, 4122.
(50) Liu, X.; Jeffries, H. E.; Sexton, K. G. *Environ. Sci. Technol.* **1999**, *33*, 4212.
(51) Tuazon, E. C.; Atkinson, R.; MacLeod, H.; Biermann, H. W.; Winer, A. M.; Carter, W. P. L.; Pitts, J. N., Jr. *Environ. Sci. Technol.* **1984**, *18*, 981.
(52) Gery, M. W.; Fox, D. L.; Jeffries, H. E. *Int. J. Chem. Kinet.* **1985**, *17*, 931.
(53) Bandow, H.; Washida, N.; Akimoto, H. *Bull. Chem. Soc. Jpn.* **1985**, *58*, 2531.
(54) *Final Report "Radical" European Commission Contract ENV4−CT97−0419*; Moortgat, G. K., Ed.; Commission of the European Communities: Brussels, Belgium, 2000.
(55) Jenkin, M. E.; Saunders, S. M.; Derwent, R. G. *Proc. Workshop on the Chem. Behaviour of Aromatic Hydrocarbons in the Troposphere*; Becker, K. H., Ed.; http://www.physchem.uni-wuppertal.de/PC−WWW_Site/workshops.html, Valencia, Spain, February 27th−29th 2000; EPFL Publishing: Lausanne, Switzerland; pp 81−87.
(56) Plum, C. N.; Sanhueza, E.; Atkinson, R.; Carter, W.; Pitts, J. N., Jr. *Environ. Sci. Technol.* **1983**, *17*, 479.